Exploring the Use of Ramsey-CPT Spectroscopy for a Microcell-Based Atomic Clock

Clément Carlé, Michael Petersen, Nicolas Passilly, Moustafa Abdel Hafiz, Emeric de Clercq, and Rodolphe Boudot

***Abstract*— We investigate the application of Ramsey spectroscopy for the development of a microcell atomic clock based on coherent population trapping (CPT). The dependence of the central Ramsey-CPT fringe properties on key experimental parameters is first studied for optimization of the clock's short-term frequency stability. The sensitivity of the clock frequency to light-shift effects is then studied. In comparison with the continuous-wave (CW) regime case, the sensitivity of the clock frequency to laser power variations is reduced by a factor up to 14 and 40.3 for dark times of 150 and 450 μs, respectively, at the expense of intensity 3.75 times higher for short-term stability optimization. The dependence of the clock frequency on the microwave power is also reduced in the Ramsey case. We demonstrate that the Ramsey-CPT interrogation improves the clock Allan deviation for averaging times higher than 100 s. With a dark time of 450 μs, a clock fractional frequency stability of 3.8×10^{-12} at 10^4 s is obtained, in comparison with the level of 8×10^{-11} obtained in the standard CW case, in similar environmental conditions. These results demonstrate that Ramsey-based interrogation protocols might be an attractive approach for the development of chip-scale atomic clocks (CSACs) with enhanced mid- and long-term stability.**

***Index Terms*— Clocks, frequency control, spectroscopy, vertical-cavity surface-emitting lasers (VCSELs).**

I. Introduction

MICROWAVE chip-scale atomic clocks (CSACs) [1]–[4] based on coherent population trapping (CPT) [5] have known a remarkable development success, including their commercialization [6], [7], and are attractive candidates for many applications such as secure communications, underwater sensor networks or GNSS-denied navigation and positioning systems. These clocks are based on an integrated physics package composed of a modulated vertical-cavity surface-emitting laser (VCSEL), optics, and an alkali vapor microfabricated cell, embedded onto a control electronics card.

For averaging times higher than 100 s, light-shift effects that originate from laser power and frequency fluctuations but also from microwave power fluctuations that impact the amplitude ratio between CPT optical sidebands [8], are known to be an important factor that affects the frequency stability of CSACs. Numerous methods have been reported to mitigate light-shift effects in CPT-based atomic clocks. A well-known method is the active stabilization of a finely tuned microwave power that nulls the sensitivity of the clock frequency to laser power variations [9]–[12]. However, the light shift suppression can become impossible when the inner-cell buffer gas pressure exceeds a certain value [13]. Other proposed methods are based on compensation for the laser frequency detuning [12], the adjustment of the cell temperature to a specific set-point [14], the fine-tuning of the laser temperature [10], the implementation of additional servo loops that reduce light-shift effects induced from variations of the laser block [7], [12], [15]–[17] or the implementation of advanced interrogation protocols based on laser power modulation sequences [18], [19].

An alternative and well-known approach to reduce light-shift effects in atomic clocks is to probe the clock transition with Ramsey spectroscopy [20]. In Ramsey-CPT spectroscopy, atoms interact with a sequence of optical CPT pulses separated by a free-evolution dark time T during which atoms do not interact with light. The theoretical modeling and experimental study of light-shifts in Ramsey-CPT spectroscopy has been investigated in several studies [21]–[26] while the demonstration of reduced sensitivity to light-shift effects has been reported in various high-performance vapor cell experiments [27]–[29].

However, to our knowledge, the Ramsey-CPT approach has been rarely explored in microcell-based atomic clocks. On the one hand, the short-term stability of a Ramsey-CPT microcell atomic clock is expected to be comparable to that obtained in the standard continuous-wave (CW) regime [30]. On the other hand, efficient and reliable generation of the CPT pulse train sequence may be challenging to implement in a miniature clock architecture since no bulky and power-consuming external modulators should be used while the laser frequency

Manuscript received March 30, 2021; accepted May 27, 2021. Date of publication June 2, 2021; date of current version September 27, 2021. This work was supported in part by the Délégation Générale de l'Armement; in part by the Région de Franche-Comté; and in part by the Agence Nationale de la Recherche (ANR) in the frame of Projects LabeX FIRST-TF under Grant ANR 10-LABX-0048, EquipX Oscillator-IMP under Grant ANR 11-EQPX-0033, and ASTRID PULSACION under Grant ANR-19-ASTR-0013-01. The work of Clément Carlé was supported in part by the Centre National des Etudes Spatiales (CNES) and in part by the Agence Innovation Défense (AID). *(Corresponding author: Rodolphe Boudot.)*

Clément Carlé, Michael Petersen, Nicolas Passilly, Moustafa Abdel Hafiz, and Rodolphe Boudot are with the Centre National de la Recherche Scientifique (CNRS), École Nationale Supérieure de Mécanique et des Microtechniques (ENSMM), University Bourgogne Franche-Comté (UBFC), University of Technology of Belfort-Montbéliard (UTBM), Franche-Comté Électronique Mécanique Thermique et Optique-Sciences et Technologies (FEMTO-ST), 25030 Besançon, France (e-mail: rodolphe.boudot@femto-st.fr).

Emeric de Clercq is with the Systèmes de Références Temps-Espace Laboratory (SYRTE), Observatoire de Paris, Université CNRS, Sorbonne Université, 75014 Paris, France.

Digital Object Identifier 10.1109/TUFFC.2021.3085249

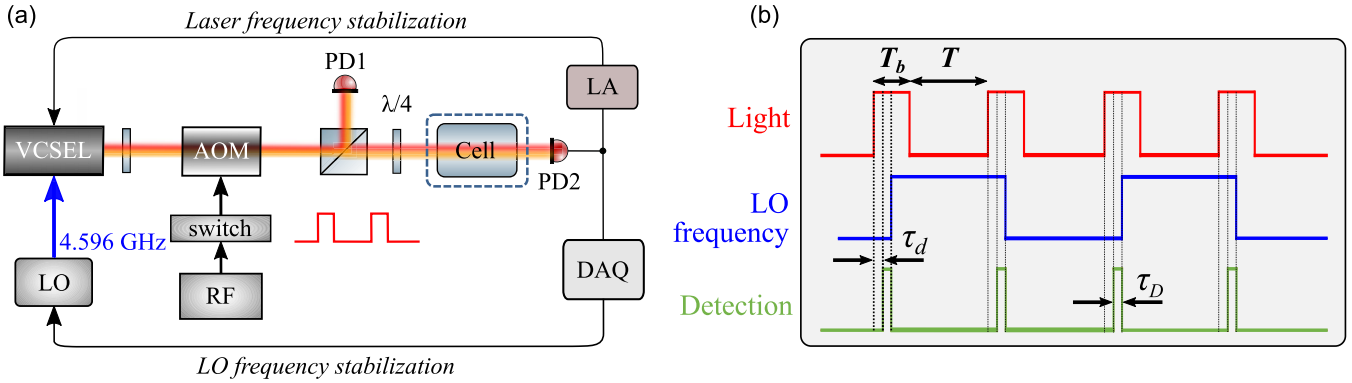

Fig. 1. (a) Architecture of the Ramsey-CPT microcell atomic clock system. Optical CPT pulses are generated at the output of a VCSEL using an external AOM. The laser power at the input of the cell is calibrated using the photodiode PD1. The light transmitted through the Cs-Ne microcell is detected by the photodiode PD2. This signal is used in two main servo loops: one for laser frequency stabilization by correcting the laser dc current, one for frequency stabilization of the microwave local oscillator (LO) source onto the CPT resonance signal. LA: lock-in amplifier. DAQ: data acquisition card. RF: radio frequency source. (b) Ramsey-CPT sequence used for clock operation. Typical sequence parameters are $T_b = 50-500$ μs, $T = 50 - 500$ μs, $\tau_d = 10$ μs, $\tau_D = 10$ μs. The microwave LO frequency is changed at each Ramsey-CPT cycle to scan both sides of the CPT resonance. Two successive signals S_1 and S_2 are used to generate the error signal and to discipline the LO frequency onto the atomic frequency.

stabilization should be managed in the pulsed regime. Technical solutions based on direct VCSEL current modulation have been explored for this purpose in the literature [31]–[33]. Nevertheless, these tests were performed with cm-scale glass blown vapor cells, giving access to longer dark times T, while no clock frequency stability results have been reported yet in the Ramsey-CPT case.

In the present article, although the pulsed CPT sequence is produced with an external acousto-optical modulator (AOM), we investigate the use of Ramsey-CPT spectroscopy in a CPT-based microcell atomic clock. In a first step, we study the dependence of main experimental parameters on the properties of the Ramsey-CPT fringe. In a second step, we measure the sensitivity of the clock frequency to variations of the laser power, the microwave power, and the dark time T of the Ramsey sequence. Comparisons with the standard CW regime are performed. A reduction of the clock frequency dependence to laser power by a factor of about 40 is obtained in the pulsed case with a dark time of 450 μs, at an expense of 3.75 times higher operation laser power. The sensitivity to microwave power variations is also reduced in the Ramsey-CPT case. The Ramsey-CPT interrogation improves the clock Allan deviation after 100 s, at the expense of degraded short-term stability when the dark time T is higher than T_2.

II. Experimental Set-Up

Fig. 1(a) describes the CPT clock experimental setup. The laser is a VCSEL tuned on the Cs D_1 line [34]. In operation, the VCSEL dc current is about 1.8 mA and the VCSEL temperature is stabilized at about 70 °C. The injection current of the VCSEL is modulated through a bias-tee at 4.596 GHz using a microwave local oscillator (LO) source (Rohde-Schwarz SMB100A) to generate two first-order optical sidebands frequency-split by 9.192 GHz for CPT interaction. The microwave power that drives the laser is noted $P_{\mu W}$. At the output of the VCSEL, the collimated beam is sent into an AOM, from which the first-order diffracted beam is isolated. This AOM is driven by a radio frequency (RF) source at 80 MHz. A high-bandwidth switch, driven by a transistor-transistor logic (TTL) sequence generated from the experiment control card, is used to turn the RF signal ON-OFF and then to produce the optical Ramsey-CPT pulsed sequence. In addition, the optical power incident in the cell P_l can be changed and controlled by adjusting the RF signal power that drives the AOM. A fraction of the light power is extracted by a beamsplitter cube and detected by the photodiode PD1. This photodiode is then used to calibrate the laser power at the cell input. After this cube, the light is circularly polarized with a quarter-wave plate and sent into a Cs vapor microfabricated cell filled with Ne buffer gas. The cell technology is comparable to the one described in [35] and [36] and no specific selection was done. From clock frequency measurements reported in Fig. 7, the Ne pressure in the cell is estimated to be 90.7 Torr at 70 °C [37]. The cell cavity where CPT interaction takes place is 2 mm in diameter and 1.4 mm in length. The laser beam diameter in the cell is 0.5 mm. In the present study, the cell temperature T_{cell} is stabilized at the mK level, experiences a static magnetic field B of 168 mG produced to isolate the 0–0 clock transition and is surrounded by a mu-metal magnetic shield to protect atoms from environmental magnetic perturbations. The laser power at the cell output is detected by the photodiode PD2. The output signal from PD2 is first used for laser frequency stabilization. For this purpose, the laser is tuned such that the two first-order sidebands are resonant with the transitions between both hyperfine levels ($F = 3$, $F = 4$) of the $6S_{1/2}$ ground state and the $F = 4$ hyperfine level of the $6P_{1/2}$ excited state of the Cs D_1 line. The laser current is sine modulated at 71 kHz, the absorption signal on the photodiode PD2 is demodulated with a lock-in amplifier (LA) and a servo amplifier [not shown in Fig. 1(a)] feeds back a correction signal onto the laser injection current to stabilize the laser frequency to the center of the Doppler-broadened optical resonance line. We note that no dedicated laser servo electronics adapted to operate in the

pulsed regime were used. A second servo-loop from PD2 is used for locking the microwave interrogation signal to the CPT resonance signal. In this case, the half-height signal on both sides of the central CPT resonance is measured by applying frequency jumps of the LO. A zero-crossing error signal is then derived by subtraction of the two measurements and used to stabilize the frequency of the microwave LO onto the CPT resonance center. The microwave source is referenced to an active hydrogen maser used as a reference for frequency shifts and stability measurements. In clock operation, the output frequency of the microwave source is digitally controlled and frequency corrections f_c (in Hz) applied to each clock cycle are recorded. The recorded values of f_c represent the frequency difference between the CPT atomic clock and the maser and thereby provide the stability of the microcell clock compared with the maser. As the maser stability is below 10^{-13} for $\tau > 1$ s [38], the measured stability stands for the microcell clock stability alone. Data acquisition, including the photodiodes' output signal, and management of the clock experiment are performed by a multi-function card connected to a computer.

Fig. 1(b) shows the typical sequence applied for operating the microcell clock in the Ramsey-CPT regime. Here, atoms interact with a sequence of optical CPT pulses of length T_b and are separated by a free-evolution dark time T. Pulses are used both for pumping the atoms into the dark state and detecting the CPT signal. The detection is performed in a window of length τ_D, after a time delay noted τ_d. In the present study, typical sequence parameters were $T_b = 50 - 500$ μs and $T = 50 - 500$ μs. τ_d and τ_D were fixed to 10 μs.

For spectroscopy and scanning of the Ramsey-CPT fringes, a dead-time of 3 ms ($\sim$10 T_2, with T_2 the hyperfine coherence relaxation time) is applied between each Ramsey cycle to ensure that most of the atoms have relaxed from the CPT state before entering a new cycle. Each fringe scan results from a total of 2000 data points, each of them derived from an average of five Ramsey cycles. For clock operation, as shown in Fig. 1(b), frequency jumps of the LO are applied at each clock cycle to probe successively both sides of the central Ramsey fringe. Two consecutive atomic signals, noted S_1 and S_2, are then used to generate the error signal $\varepsilon = S_2 - S_1$ required for the LO frequency stabilization loop.

III. Ramsey-CPT Spectroscopy

This section reports the impact of main experimental parameters onto the central Ramsey-CPT fringe characteristics, including its full-width at half maximum (FWHM), its signal S defined as its peak-to-peak amplitude and its contrast C defined as the ratio between the fringe signal and the dc background at half-height of the fringe. This study permits to identify how to maximize the contrast/FWHM ratio, known as a figure of merit to optimize the shot-noise limited clock short-term frequency stability, in the CW [39] or Ramsey regimes [40]. In the CW case, the contrast C is defined as the ratio between the CPT resonance amplitude and its dc background level. For illustration, Fig. 2 shows a typical clock signal in the standard CW and Ramsey-CPT cases. In the

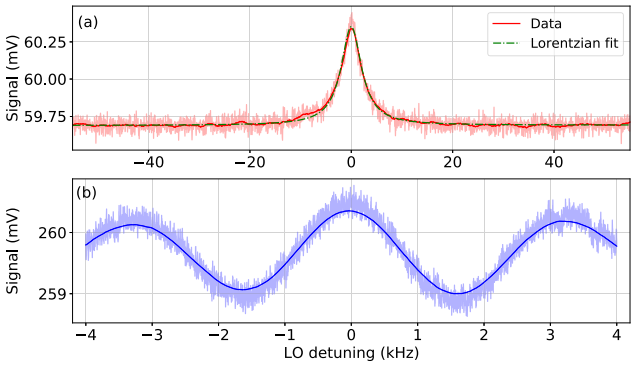

Fig. 2. (a) CPT resonance obtained in the standard CW and (b) central Ramsey-CPT fringes detected in the pulsed case. Note that x-scales are different in (a) and (b). In the CW case, experimental parameters are $T_{\text{cell}} = 78$ °C, $P_l = 12$ μW and $P_{\mu\text{W}} = -1$ dBm. The resonance is fit by a Lorentzian function shown in a dashed-dotted green line. In the Ramsey-CPT case, experimental parameters are $T_{\text{cell}} = 70$ °C, $P_l = 45$ μW and $P_{\mu\text{W}} = -1$ dBm, $T_b = 150$ μs and $T = 260$ μs. Raw (lighter-colored curves) and averaged spectra (solid lines) are shown. The averaged curves are obtained by applying a 80-point (200-point) rolling average to raw data, for curves (a) and (b), respectively.

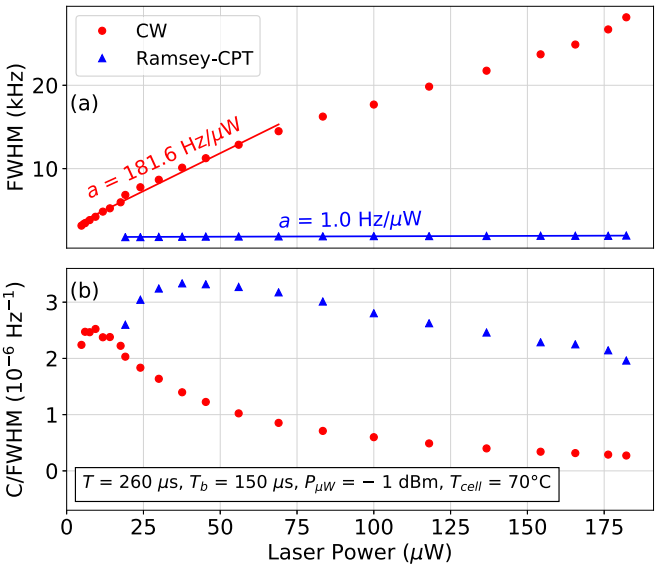

Fig. 3. (a) FWHM and (b) C/FWHM of the central Ramsey-CPT fringe versus the total laser power incident in the cell. The beam diameter is 0.5 mm. Measurements performed in the CW regime, under the same conditions, are reported for comparison. Experimental parameters are given in the figure. Solid lines in (a) indicate a linear fit function to the data.

CW case, the CPT resonance is correctly fit by a Lorentzian function with an FWHM of 4.8 kHz. The resonance contrast is 1.27%. The Ramsey-CPT fringe shown in Fig. 2(b) exhibits a linewidth of 1.8 kHz and a contrast of 0.46%.

Fig. 3 displays the FWHM and the contrast/FWHM figure of the CPT resonance (CW case) or the Ramsey-CPT central fringe, as a function of the laser power. Results are compared with those obtained in the CW case. We observe in Fig. 3(a) only a slight power broadening of the central fringe, with a slope of about 1 Hz/μW. For comparison, in the CW regime, this coefficient is about 181.6 Hz/μW in the

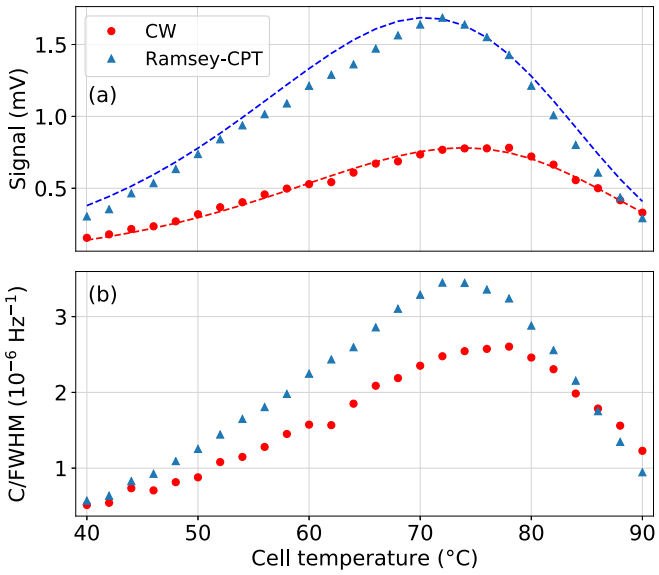

Fig. 4. (a) Signal and (b) C/FWHM of the clock resonance in the CW and Ramsey-CPT cases versus the cell temperature. In the CW case, experimental parameters are $P_l = 12$ μW and $P_{\mu W} = -1$ dBm. In the Ramsey-CPT case, experimental parameters are: $T_b = 150$ μs, $T = 260$ μs, $P_{\mu W} = -1$ dBm and $P_l = 45$ μW. In (a), experimental data are approximated by a simple phenomenological model (see the text for details), shown as a dashed line.

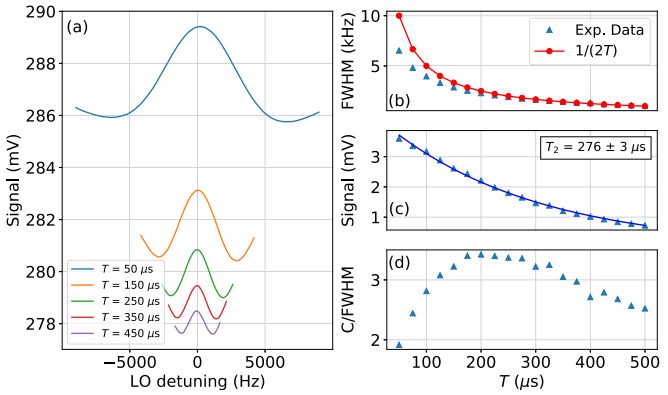

Fig. 5. (a) Ramsey-CPT fringes detected in the Cs-Ne microfabricated cell for different values of the dark time T. Experimental parameters are $T_{cell} = 70$ °C, $P_l = 45$ μW, $P_{\mu W} = -1$ dBm, $T_b = 150$ μs. (b) FWHM, (c) signal, and (d) C/FWHM of the central fringe versus the dark time T. In (b), experimental data and the expected $1/(2T)$ dependence is shown. In (c), experimental data are fit by an exponential decay function, shown as a solid line. In (d), the C/FWHM is in units of 10^{-6} Hz^{-1}.

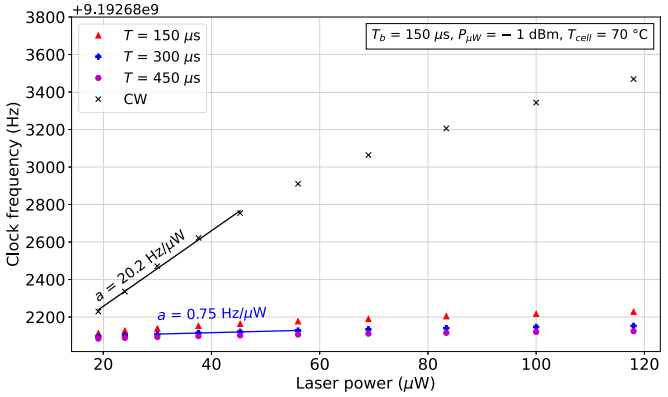

Fig. 6. Clock frequency versus the laser power, with Ramsey-CPT interrogation, for three different values of the dark time T (150, 300 and 450 μs). Experimental parameters are: $T_b = 150$ μs, $P_{\mu W} = -1$ dBm and $T_{cell} = 70$ °C. A measurement performed in the CW regime, for the same cell temperature and microwave power, is shown for comparison.

10–75-μW range, for the same cell temperature (70 °C) and microwave power (−1 dBm). In Fig. 3(b), we note that the C/FWHM ratio is maximized in the Ramsey-CPT case for a laser power of about 45 μW, here at a value of about 3.2×10^{-6} Hz^{-1}. In the CW regime, the optimal C/FWHM is found to be 30% lower and for a power of about 12 μW.

Fig. 4 shows the signal (a) and the C/FWHM ratio (b) of the clock resonance in both the CW and the Ramsey-CPT cases versus the cell temperature. The temperature dependence of dark resonances was studied in [41]. In this study, the drop of the CPT signal above a given cell temperature value was explained by a simple model based on the temperature dependence of the Cs density and the vapor optical thickness. In the present study, a simple phenomenological model similar to the one exposed in [41] was developed to predict the temperature dependence of the atomic signal. This model was extended to the Ramsey case by multiplying the CW signal by a relaxation term exp $(-\gamma_c T)$, with γ_c the temperature-dependent relaxation rate of the hyperfine coherence. The relaxation scales as the temperature, due mainly to the increasing spin-exchange collision rate. The only adjustable parameters are the proportionality coefficient between the absorption coefficient, the Cs density and the maximum amplitude for the CW-case curve, and the maximum amplitude for the Ramsey-case curve. Results derived from the model are shown as dashed lines in Fig. 4(a). A correct agreement is found between experimental data and the model. In Fig. 4, the CPT signal shows a maximum around 76 °C in the CW case for a laser power of 12 μW. We observed that the position of this maximum signal was shifted at slightly higher temperatures with increased laser power. This behavior was observed and explained in [42]. In the Ramsey-CPT case, the clock resonance signal is maximized at a lower cell temperature of about 71 °C. This difference is explained by the relaxation of the hyperfine coherence during the free evolution time of the Ramsey interrogation.

Fig. 5(a) shows the central Ramsey-CPT fringe detected in the Cs-Ne microfabricated cell, for different values of the dark time T, for a laser power of 45 μW. The Ramsey-CPT fringe signal and dc level decrease with an increased value of the dark time since atoms relax freely during a longer time [43]. In Fig. 5(b), we observe that the FWHM of the central fringe is narrower than the expected Ramsey $1/(2T)$ linewidth, for T values lower than 300 μs. This phenomenon was already observed in [28] and is explained in [44]. By fitting the fringe signal-versus-T dependence [shown in Fig. 5(c)] by an exponential decay function, we extract a CPT coherence lifetime T_2 of 276 ± 3 μs. In Fig. 5(d), we see that the contrast/FWHM ratio is maximized for a T value in the 200–300-μs range, i.e., for $T \sim T_2$, as usually observed in high-performance vapor cell clocks [28], [40].

IV. Light-Shift Measurements

We performed light-shift measurements of the Ramsey-CPT microcell atomic clock. In the first step, light shifts induced by discrete changes in the AOM driving power and then of the laser power entering in the microcell are applied while the clock is continuously running. Fig. 6 reports the clock frequency versus the total laser power incident onto the cell, for three different values of the free-evolution time T.

Non-linear light-shift trends are clearly observed, with higher slopes for power values lower than about 60 μW. Around the 45-μW laser power range, where the clock short-term stability is optimized in the Ramsey-CPT case (see Fig. 3), the light-shift coefficients are 1.5, 0.75, and 0.50 Hz/μW for T values of 150, 300, and 450 μs, respectively. For comparison, a light-shift measurement performed in the CW regime, in identical experimental conditions (cell temperature, microwave power, same connected excited state), yields at low power values a light-shift slope of about 20.2 Hz/μW, i.e., a factor 14 and 40.3 higher than in the pulsed case, for dark times of 150 and 450 μs, respectively. However, note again that when the clock is operated with a Rabi interrogation, the short-term frequency stability is optimized with a laser power of about 12 μW (see Fig. 3), and then typical laser power fluctuations are about $45/12 = 3.75$ times smaller. Thus, for $T = 450$ μs, an overall laser power shift reduction factor of about $40.3/3.75 \sim 10.7$ is expected with the Ramsey-CPT scheme. The latter is reduced to 3.7 and 7.1 for T values of 150 and 300 μs, respectively.

As reported in Fig. 7, we also studied experimentally the impact of the pulse duration length T_b onto the clock frequency. Again, for these measurements, the clock is locked continuously. Laser power jumps are suddenly applied and the steady-state average output clock frequency is recorded after waiting for a few minutes.

In Ramsey-CPT spectroscopy, the light shift is related to the dark state pumping rate. Theoretical studies predict a faster reduction in the light shift with the increase of the pumping pulse duration T_b [21], [24], [45]. This prediction is mainly attributed to the fact that longer pumping pulses help to create complete dark states and was confirmed in a cold-atom CPT clock [22], [24]. This behavior is observed in Fig. 7(b) where a slight reduction of the light-shift absolute value is observed at the highest value of T_b. Nevertheless, in comparison with [22], [24], note that our tests are performed in a miniature buffer-gas-filled Cs vapor cell that operates at high alkali density and buffer gas pressure. The presence of buffer gas implies a significant broadening of the optical lines and a non-negligible mixing of excited states. Thus, a dedicated theoretical and experimental study would be needed to analyze and understand in more detail results obtained in our conditions. This study is not treated in the frame of the present article. For frequency stability concerns, we note that the light-shift coefficient is comparable for all values of T_b in Fig. 7(a).

We measured in Fig. 8 the clock frequency versus the laser power, for different values of the microwave power, in the Ramsey-CPT case. Measurements were performed with $T_b = 150$ μs and $T = 260$ μs.

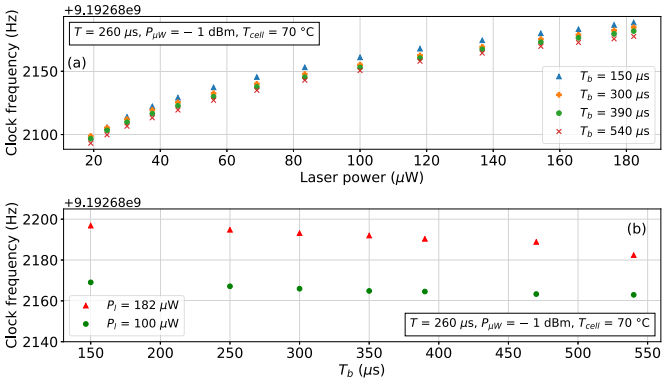

Fig. 7. (a) Clock frequency versus the laser power, with Ramsey-CPT interrogation, for different values of the bright time T_b (150, 300, 390, and 540 μs), with $T = 260$ μs. Experimental parameters are $P_{\mu W} = -1$ dBm and $T_{cell} = 70$ °C. (b) Clock frequency versus T_b for two different laser power values (182 and 100 μW).

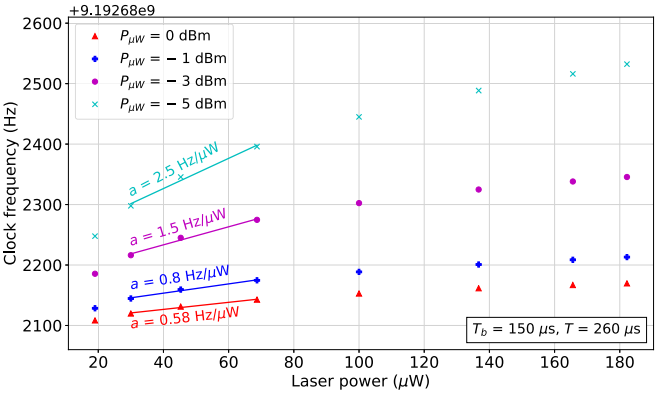

Fig. 8. Clock frequency versus the laser power, with Ramsey-CPT interrogation, for different values of the microwave power $P_{\mu W}$ (0, −1, −3, and −5), with T= 260 μs, $T_b = 150$ μs, and $T_{cell} = 70$ °C.

We observe that the light-shift coefficient a is reduced with increased microwave power. Let us underline that none of the microwave power levels in the tested range allows canceling the light-shift slope, neither in the Ramsey-CPT nor the CW regime. The latter was also not observed in the CW regime. The difficult detection of such a magic microwave power might be due to the non-negligible value of the buffer gas pressure in the cell [13]. In the CW case, a residual light-shift coefficient of +6.4 Hz/μW was measured at $P_{\mu W} = 0$ dBm. This value is 11 times higher than the one obtained in the pulsed case with $P_{\mu W} = 0$ dBm.

An alternative and straightforward way to illustrate the dependence of the clock frequency on microwave power variations is given in Fig. 9. In this experiment, the sensitivity of the clock frequency is increased from −24 Hz/dB at a laser power of 24 μW to −79.2 Hz/dB at 182 μW. For comparison, a measurement performed in the CW regime for a laser power of 12 μW (close to the power that optimizes the clock short-term stability in the CW case) yielded a sensitivity to microwave power of about −126 Hz/dB. This result demonstrates that the Ramsey-CPT spectroscopy leads

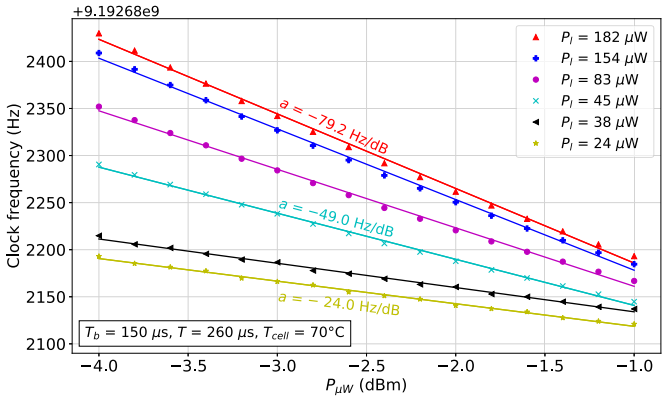

Fig. 9. Clock frequency versus the microwave power, with Ramsey-CPT interrogation, for different values of the laser power, with $T = 260$ μs, $T_b = 150$ μs and $T_{\text{cell}} = 70$ °C.

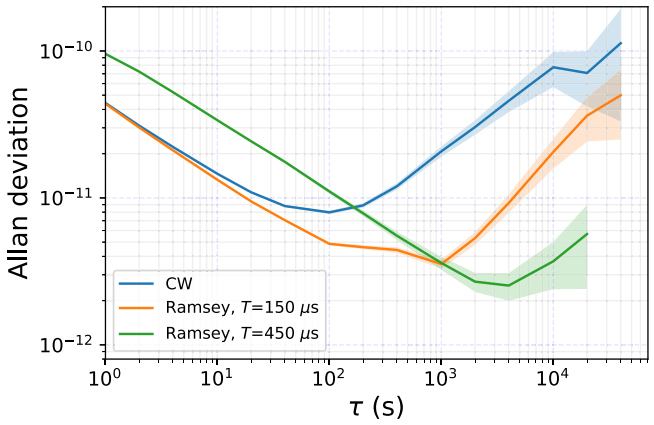

Fig. 10. Allan deviation of the clock frequency in the Ramsey-CPT case, for two different values of the dark time T (150 and 450 μs). Experimental parameters are: $P_{\mu W} = -1$ dBm, $T_b = 250$ μs, $T_{\text{cell}} = 70$ °C, $\tau_d = 10$ μs, $\tau_D = 10$ μs. A measurement obtained in the CW regime with the same setup, with $P_{\mu W} = -1$ dBm and $T_{\text{cell}} = 70$ °C, is given for comparison. The laser intensity at the cell input is 55 and 196 μW/mm^2, for the CW and Ramsey cases, respectively.

to a reduction of the clock frequency sensitivity to microwave power variations, despite the use of short dark times of a few hundreds of microseconds.

V. Frequency Stability Results

In Section V, clock frequency stability measurements were performed, both in the CW and Ramsey-CPT cases. For these measurements, the beam diameter was increased to about 1.0 mm. In both CW and Ramsey cases, the laser intensity was adjusted before running the clock to be comparable to the one obtained in Fig. 3(b) for optimized short-term stability [CW: 55 μW/mm^2, for 61 μW/mm^2 in Fig. 3(b), Ramsey: 196 μW/mm^2, for 229 μW/mm^2 in Fig. 3(b)]. During these measurements, some experimental parameters such as the input laser power or the microwave power were not routinely recorded, preventing the establishment of a detailed clock mid-term stability budget. However, for all tests mentioned below, we confirm that the clock setup ran in comparable environmental conditions. The microwave power is −1 dBm and the cell temperature is 70 °C in all tests.

Fig. 10 shows the Allan deviation of the clock frequency, using Ramsey-CPT interrogation, for two different values of the dark time T (150 or 450 μs). A measurement performed in the CW regime is shown for comparison. In the CW regime, the clock short-term frequency stability is 4.2×10^{-11} at 1 s and 8×10^{-12} at 100 s. After 100 s, the clock Allan deviation is degraded to reach 8×10^{-11} at 10^4 s. These performances at 10^4 s are in the same order as the ones reported in previous studies when no light-shift mitigation techniques are applied [16]. In the Ramsey-CPT case, for $T = 150$ μs, the clock Allan deviation at 1 s is comparable to that obtained in the CW case but integrates better to reach 3.5×10^{-12} at 10^3 s, before degradation at the level of 2×10^{-11} at 10^4 s. Note that the improvement factor (4) of the clock stability at 10^4 s in this case, in comparison with the CW regime, is in correct agreement with the overall light-shift reduction factor of 3.7 mentioned in Section IV for this T value. For $T = 450$ μs, the short-term stability of the clock is degraded to 9×10^{-11} $\tau^{-1/2}$. Such degradation, experienced when $T = 450$ μs compared to $T = 150$ μs, was expected from the signal reduction [see Fig. 3(c)] due to the increased relaxation of the CPT coherence. At the same time, due to the increased value of T, a significant improvement of the clock mid-term frequency stability, reaching 3.8×10^{-12} at 10^4 s, is obtained. Here, the improvement factor (∼21) of the clock stability at 10^4 s in comparison with the CW regime is about two times higher than the overall light-shift reduction factor of 10.7 measured in Section IV for this T value. In the latter case, the clock stability after 10^4 s is still limited by another process. The cause of this limitation is unknown to date and will require further investigations.

VI. Conclusion

In conclusion, we have investigated the application of Ramsey-CPT spectroscopy for a CPT-based microcell atomic clock using a VCSEL laser. An external AOM was used to produce the optical CPT pulses. The influence of key experimental parameters onto the central Ramsey-CPT fringe properties was investigated for optimization of the clock short-term stability and compared with some results obtained in the CW case. The impact of the laser power, the microwave power and the free evolution dark time onto the clock frequency was studied. A reduction of the clock frequency sensitivity to laser power variations by a factor of about 40 was measured, compared to the standard CW case, with a dark time T of 450 μs. We measured that the clock frequency dependence to microwave power variations is also reduced with Ramsey-CPT spectroscopy. A slight reduction of the light-shift absolute value with increased length of the light pulses was observed. The value of T_b did not change significantly the light-shift coefficient. For a dark time T of 150 μs, the clock short-term stability, at the level of 4.2×10^{-11} $\tau^{-1/2}$, is similar to the one obtained in the CW case. For $T = 450$ μs, the clock exhibits a degraded short-term stability at the level of 9×10^{-11} at 1 s but is improved for $\tau > 200$ s, reaching the level of 3.8×10^{-12} at 10^4 s, instead of 8×10^{-11} in the CW case and 2×10^{-11} with $T = 150$ μs. These results at 10^4 s demonstrate that the use of Ramsey-CPT spectroscopy might

be an attractive solution for the development of miniaturized atomic clocks with improved mid-term stability. Obviously, alternative techniques, such as the modulation of the laser current [31]–[33], will have to be implemented to prevent the use of an external AOM and keep a simple clock architecture easier to miniaturize. In addition, the exploration of advanced Ramsey interrogation protocols [46], [47], [47]–[50], proven to be efficient in high-performance vapor cell clocks for enhanced mitigation of light-shift effects, might be also of interest.

ACKNOWLEDGMENT

The authors acknowledge P. Abbé and G. Martin (Franche-Comté Électronique Mécanique Thermique et Optique-Sciences et Technologies (FEMTO-ST), Besançon, France) for their help with the experimental setup and electronics and Edouard Feingesicht for his valuable contribution to the model developments. The authors thank the platform Oscillator-Imp for the distribution of a reference hydrogen maser signal in the laboratory, used to characterize the CPT clock performances, and the platform MIMENTO used for the development of the microfabricated cell.

REFERENCES

[1] S. Knappe *et al.*, "A microfabricated atomic clock," *Appl. Phys. Lett.*, vol. 85, no. 9, pp. 1460–1462, Aug. 2004.

[2] S. Knappe, "MEMS atomic clocks," in *Comprehensive Microsystems*, Y. B. Gianchandani, O. Tabata, and H. Zappe, Eds. Oxford, U.K.: Elsevier, 2008, pp. 571–612.

[3] J. Kitching, "Chip-scale atomic devices," *Appl. Phys. Rev.*, vol. 5, no. 3, Sep. 2018, Art. no. 031302.

[4] H. Zhang *et al.*, "ULPAC: A miniaturized ultralow-power atomic clock," *IEEE J. Solid-State Circuits*, vol. 54, no. 11, pp. 3135–3148, Nov. 2019.

[5] J. Vanier, "Atomic clocks based on coherent population trapping: A review," *Appl. Phys. B, Lasers Opt.*, vol. 81, no. 4, pp. 421–442, Aug. 2005.

[6] R. Lutwak *et al.*, "The chip-scale atomic clock-prototype evaluation," in *Proc. 39th Annu. Precise Time Time Interval Meeting*, Long Beach, CA, USA, 2007, pp. 269–290.

[7] R. Lutwak *et al.*, "The miniature atomic clock–pre-production results," in *Proc. IEEE Int. Freq. Control Symp. Joint 21st Eur. Freq. Time Forum*, May 2007, pp. 1327–1333.

[8] Y. Yin, Y. Tian, Y.-C. Wang, and S.-H. Gu, "The light shift of a chip-scale atomic clock affected by asymmetrical multi-chromatic laser fields," *Spectrosc. Lett.*, vol. 50, no. 4, pp. 227–231, Apr. 2017.

[9] M. Zhu and L. S. Cutler, "Theoretical and experimental study of light shift in a CPT-based Rb vapor cell frequency standard," in *Proc. 32nd Annu. Precise Time Time Interval (PTTI) Meeting*, 2000, pp. 311–323.

[10] V. Shah, V. Gerginov, P. D. D. Schwindt, S. Knappe, L. Hollberg, and J. Kitching, "Continuous light-shift correction in modulated coherent population trapping clocks," *Appl. Phys. Lett.*, vol. 89, no. 15, Oct. 2006, Art. no. 151124.

[11] B. H. McGuyer, Y.-Y. Jau, and W. Happer, "Simple method of light-shift suppression in optical pumping systems," *Appl. Phys. Lett.*, vol. 94, no. 25, Jun. 2009, Art. no. 251110.

[12] Y. Zhang, W. Yang, S. Zhang, and J. Zhao, "Rubidium chip-scale atomic clock with improved long-term stability through light intensity optimization and compensation for laser frequency detuning," *J. Opt. Soc. Amer. B, Opt. Phys.*, vol. 33, no. 8, pp. 1756–1763, 2016.

[13] M. I. Vaskovskaya, E. A. Tsygankov, D. S. Chuchelov, S. A. Zibrov, V. V. Vassiliev, and V. L. Velichansky, "Effect of the buffer gases on the light shift suppression possibility," *Opt. Exp.*, vol. 27, no. 24, pp. 35856–35864, 2019.

[14] D. Miletic, C. Affolderbach, M. Hasegawa, R. Boudot, C. Gorecki, and G. Mileti, "AC stark-shift in CPT-based cs miniature atomic clocks," *Appl. Phys. B, Lasers Opt.*, vol. 109, no. 1, pp. 89–97, Oct. 2012.

[15] J. Deng, J. D. Crockett, and T. C. English, "Light stabilization for an optically excitable atomic medium," U.S. Patent 6 927 636 B2, Aug. 9, 2005. [Online]. Available: https://patents.google.com/patent/US6927636B2/en

[16] R. Vicarini *et al.*, "Mitigation of temperature-induced light-shift effects in miniaturized atomic clocks," *IEEE Trans. Ultrason., Ferroelectr., Freq. Control*, vol. 66, no. 12, pp. 1962–1967, Dec. 2019.

[17] S. Yanagimachi, K. Harasaka, R. Suzuki, M. Suzuki, and S. Goka, "Reducing frequency drift caused by light shift in coherent population trapping-based low-power atomic clocks," *Appl. Phys. Lett.*, vol. 116, no. 10, Mar. 2020, Art. no. 104102.

[18] V. I. Yudin *et al.*, "General methods for suppressing the light shift in atomic clocks using power modulation," *Phys. Rev. Appl.*, vol. 14, no. 2, Aug. 2020, Art. no. 024001.

[19] M. Abdel Hafiz *et al.*, "Protocol for light-shift compensation in a continuous-wave microcell atomic clock," *Phys. Rev. Appl.*, vol. 14, no. 3, Sep. 2020, Art. no. 034015.

[20] N. F. Ramsey, "A molecular beam resonance method with separated oscillating fields," *Phys. Rev.*, vol. 78, no. 6, p. 695, 1950.

[21] P. R. Hemmer, M. S. Shahriar, V. D. Natoli, and S. Ezekiel, "AC stark shifts in a two-zone Raman interaction," *J. Opt. Soc. Amer. B, Opt. Phys.*, vol. 6, no. 8, p. 1519, 1989.

[22] X. Liu, E. Ivanov, V. I. Yudin, J. Kitching, and E. A. Donley, "Low-drift coherent population trapping clock based on laser-cooled atoms and high-coherence excitation fields," *Phys. Rev. Appl.*, vol. 8, no. 5, Nov. 2017, Art. no. 054001.

[23] J. W. Pollock *et al.*, "AC stark shifts of dark resonances probed with Ramsey spectroscopy," *Phys. Rev. A, Gen. Phys.*, vol. 98, no. 5, Nov. 2018, Art. no. 053424.

[24] M. Shuker, J. W. Pollock, V. I. Yudin, J. Kitching, and E. A. Donley, "Optical pumping, decay rates and light shifts of cold-atom dark states," 2019, *arXiv:1909.02649*. [Online]. Available: http://arxiv.org/abs/1909.02649

[25] Y. Yano, W. Gao, S. Goka, and M. Kajita, "Theoretical and experimental investigation of the light shift in Ramsey coherent population trapping," *Phys. Rev. A, Gen. Phys.*, vol. 90, no. 1, Jul. 2014, Art. no. 013826.

[26] T. Zanon-Willette, E. de Clercq, and E. Arimondo, "Ultrahigh-resolution spectroscopy with atomic or molecular dark resonances: Exact steady-state line shapes and asymptotic profiles in the adiabatic pulsed regime," *Phys. Rev. A, Gen. Phys.*, vol. 84, no. 6, Dec. 2011, Art. no. 062502.

[27] N. Castagna, R. Boudot, S. Guérandel, E. de Clercq, N. Dimarcq, and A. Clairon, "Investigations on continuous and pulsed interrogation for a CPT atomic clock," *IEEE Trans. Ultrason., Ferroelectr., Freq. Control*, vol. 56, no. 2, pp. 246–253, Feb. 2009.

[28] M. Abdel Hafiz, G. Coget, P. Yun, S. Guérandel, E. de Clercq, and R. Boudot, "A high-performance Raman–Ramsey Cs vapor cell atomic clock," *J. Appl. Phys.*, vol. 121, no. 10, Mar. 2017, Art. no. 104903.

[29] S. Micalizio, A. Godone, F. Levi, and C. Calosso, "Medium-long term frequency stability of pulsed vapor cell clocks," *IEEE Trans. Ultrason., Ferroelectr., Freq. Control*, vol. 57, no. 7, pp. 1527–1534, Jul. 2010.

[30] R. Boudot, V. Maurice, C. Gorecki, and E. de Clercq, "Pulsed coherent population trapping spectroscopy in microfabricated Cs–Ne vapor cells," *J. Opt. Soc. Amer. B, Opt. Phys.*, vol. 35, no. 5, pp. 1004–1010, 2018.

[31] Y. Yano, S. Goka, and M. Kajita, "Two-step pulse observation for Raman–Ramsey coherent population trapping atomic clocks," *Appl. Phys. Exp.*, vol. 8, no. 1, Jan. 2015, Art. no. 012801.

[32] T. Ide, S. Goka, and Y. Yano, "CPT pulse excitation method based on VCSEL current modulation for miniature atomic clocks," in *Proc. Joint Conf. IEEE Int. Freq. Control Symp. Eur. Freq. Time Forum*, Denver, CO, USA, Apr. 2015, pp. 269–290.

[33] M. Fukuoka, D. Haraguchi, and S. Goka, "Light shift characteristics of Ramsey-coherent population trapping resonances excited by two-step drive current," in *Proc. Int. Freq. Control Symp., Eur. Freq. Time Forum Joint Meeting*, Orlando, FL, USA, 2019, pp. 269–290.

[34] E. Kroemer *et al.*, "Characterization of commercially available vertical-cavity surface-emitting lasers tuned on Cs D_1 line at 894.6 nm for miniature atomic clocks," *Appl. Opt.*, vol. 55, no. 31, pp. 8839–8847, 2016.

[35] M. Hasegawa *et al.*, "Microfabrication of cesium vapor cells with buffer gas for MEMS atomic clocks," *Sens. Actuators A, Phys.*, vol. 167, no. 2, pp. 594–601, Jun. 2011.

[36] R. Vicarini *et al.*, "Demonstration of the mass-producible feature of a Cs vapor microcell technology for miniature atomic clocks," *Sens. Actuators A, Phys.*, vol. 280, pp. 99–106, Sep. 2018.

[37] O. Kozlova, S. Guérandel, and E. de Clercq, "Temperature and pressure shift of the Cs clock transition in the presence of buffer gases: Ne, N2, Ar," *Phys. Rev. A, Gen. Phys.*, vol. 83, no. 6, Jun. 2011, Art. no. 062714.

[38] *The Datasheet of the Hydrogen Maser*. [Online]. Available: htt.ps://w.w.w.t4science.com/products/imaser3000/

[39] V. Shah and J. Kitching, "Advances in coherent population trapping for atomic clocks," *Adv. At., Mol., Opt. Phys.*, vol. 59, pp. 21–74, Jan. 2010.
[40] S. Micalizio, C. E. Calosso, A. Godone, and F. Levi, "Metrological characterization of the pulsed Rb clock with optical detection," *Metrologia*, vol. 49, no. 4, pp. 425–436, Aug. 2012.
[41] S. Knappe, J. Kitching, L. Hollberg, and R. Wynands, "Temperature dependence of coherent population trapping resonances," *Appl. Phys. B, Lasers Opt.*, vol. 74, no. 3, pp. 217–222, Mar. 2002.
[42] O. Kozlova, J.-M. Danet, S. Guerandel, and E. de Clercq, "Limitations of long-term stability in a coherent population trapping Cs clock," *IEEE Trans. Instrum. Meas.*, vol. 63, no. 7, pp. 1863–1870, Jul. 2014.
[43] R. Boudot, S. Guérandel, E. de Clercq, N. Dimarcq, and A. Clairon, "Current status of a pulsed CPT Cs cell clock," *IEEE Trans. Instrum. Meas.*, vol. 58, no. 4, pp. 1217–1222, Apr. 2009.
[44] J. Vanier and C. Audoin, *The Quantum Physics of Atomic Frequency Standards*, vol. 2. Philadelphia, PA, USA: Adam Hilger, 1989.
[45] M. S. Shahriar, P. R. Hemmer, D. P. Katz, A. Lee, and M. G. Prentiss, "Dark-state-based three-element vector model for the stimulated Raman interaction," *Phys. Rev. A, Gen. Phys.*, vol. 55, no. 3, pp. 2272–2282, Mar. 1997.
[46] C. Sanner, N. Huntemann, R. Lange, C. Tamm, and E. Peik, "Autobalanced Ramsey spectroscopy," *Phys. Rev. Lett.*, vol. 120, no. 5, Jan. 2018, Art. no. 053602.
[47] M. Abdel Hafiz *et al.*, "Symmetric autobalanced Ramsey interrogation for high-performance coherent-population-trapping vapor-cell atomic clock," *Appl. Phys. Lett.*, vol. 112, no. 24, Jun. 2018, Art. no. 244102.
[48] M. Shuker *et al.*, "Ramsey spectroscopy with displaced frequency jumps," *Phys. Rev. Lett.*, vol. 122, no. 11, Mar. 2019, Art. no. 113601.
[49] M. Shuker *et al.*, "Reduction of light shifts in Ramsey spectroscopy with a combined error signal," *Appl. Phys. Lett.*, vol. 114, no. 14, Apr. 2019, Art. no. 141106.
[50] M. Y. Basalaev, V. I. Yudin, D. V. Kovalenko, T. Zanon-Willette, and A. V. Taichenachev, "Generalized Ramsey methods in the spectroscopy of coherent-population-trapping resonances," *Phys. Rev. A, Gen. Phys.*, vol. 102, no. 1, Jul. 2020, Art. no. 013511.

Clément Carlé received the Engineer Diploma degree from the École Nationale Supérieure de Mécanique et des Microtechniques (ENSMM), Besançon, France, in 2020. He is currently pursuing the Ph.D. degree with the Franche-Comté Électronique Mécanique Thermique et Optique-Sciences et Technologies (FEMTO-ST), Besançon, with a thesis on the topic of miniaturized atomic clocks based on coherent population trapping (CPT).

Michael Petersen received the Ph.D. degree in physical sciences from Université Pierre et Marie Curie, Paris, France, in 2009.

From 2009 to 2011, he was a Postdoctoral Researcher with BIPM, Sèvres, France, working on ozone laser spectroscopy. He was with the Imperial College London, London, U.K., from 2011 to 2013, to work on cold molecules experiments. From 2013 to 2015, he was a Postdoctoral Researcher with the Université de Neuchâtel, Neuchatel, Switzerland, working on atomic fountains. Since 2016, he has been working with the Time-Frequency Department, Franche-Comté Électronique Mécanique Thermique et Optique-Sciences et Technologies (FEMTO-ST), Besançon, France, contributing to the development of compact and miniaturized vapor cell atomic clocks.

Nicolas Passilly received the M.S. degree in physics and the Ph.D. degree in laser physics from the University of Caen, Caen, France, in 2002 and 2005, respectively.

From 2006 to 2008, he was a Postdoctoral Researcher with the University of Eastern Finland, Joensuu, Finland. In 2008, he joined the Franche-Comté Électronique Mécanique Thermique et Optique-Sciences et Technologies (FEMTO-ST), Besançon, France, where he became a CNRS Scientist in 2010 and is currently a Senior Researcher with the Centre National de la Recherche Scientifique (CNRS). His research interests include micro-optics and microoptoelectromechanical systems (MOEMS) devices.

Moustafa Abdel Hafiz received the Ph.D. degree from Université Bourgogne-Franche-Comté, Besançon, France, in 2017. His Ph.D. thesis work, led at the Franche-Comté Électronique Mécanique Thermique et Optique-Sciences et Technologies (FEMTO-ST), Besançon, was focused on the development of a high-performance microwave Cs vapor cell atomic clock based on coherent population trapping (CPT).

From March 2018 to end 2019, he has worked as a Postdoctoral Researcher with Physikalisch-Technische Bundesanstalt (PTB), Braunschweig, Germany, on the development of a transportable Yb^+ ion optical clock (Opticlock). Since January 2020, he has been a Permanent Assistant Professor with the École Nationale Supérieure de Mécanique et des Microtechniques (ENSMM), doing his research activities at FEMTO-ST. He is mainly involved in the development of a single Yb^+ trapped-ion optical clock and vapor cell atomic clocks.

Emeric de Clercq received the Ph.D. degree from Paris-Sud University, Orsay, France, in 1980.

Since 1982, he has been with Laboratoire National de Métrologie et d'Essais—Systèmes de Références Temps-Espace (LNE-SYRTE), Observatoire de Paris, Paris, France. He has been in charge of the cesium beam primary frequency standard project and involved in the development of compact vapor cell atomic clocks.

Rodolphe Boudot received the Ph.D. degree in engineering sciences from the Université de Franche-Comté, Besançon, France, in 2006.

From 2007 to 2009, he was a Postdoctoral Researcher with the Systèmes de Références Temps-Espace Laboratory (SYRTE), Paris, France. Since October 2008, he has been a Permanent CNRS Researcher with the Franche-Comté Électronique Mécanique Thermique et Optique-Sciences et Technologies (FEMTO-ST). Since January 2017, he has been the Head of the OHMS Group, Time-Frequency Department, FEMTO-ST. From April 2018 to July 2019, he has worked as a NIST Guest Researcher with the Atomic Devices and Instrumentation (ADI) Group, Boulder, CO, USA, on laser cooling experiments in microfabricated cells, cold-atom clocks and sensors. His research interests include compact and miniature cell atomic clocks, low noise electronics, oscillators, frequency synthesizers, and laser spectroscopy.